Plasma Induced Damage Reduction of Ultra Low-k Dielectric by Using Source Pulsed Plasma Etching for Next BEOL Interconnect Manufacturing

Jun Ki Jang, Hyun Woo Tak, Ye Ji Shin, Doo San Kim, and Geun Young Yeom

***Abstract*—In order to reduce the interconnect resistance and capacitance (RC) time delay of a semiconductor integrated circuit, a more porous dielectric material is used in recent interconnection for lower dielectric constant. However, it is difficult to use highly porous low-k dielectric materials at the narrow pitch because it is easily damaged during the plasma etching processes. In this study, as one of the plasma induced damage reduction methods in the etching of porous low-k dielectric, RF pulsed plasma methods have been investigated by using a dual frequency capacitively coupled plasma etching system. RF pulsed plasmas generated more polymerizing species and less UV compared to continuous wave plasmas and showed reduced damaged layer compared to the conventional continuous wave plasma etching. Porous SiCOH dielectric patterned with a TiN hard mask was etched using the RF pulsed plasmas and the results showed more anisotropic etching profiles with less sidewall damages, which was estimated by the thickness loss of sidewall low-k material after dipping into a diluted HF solution. Therefore, it is believed that the RF pulsed plasma etching process of ultra low-k dielectric materials can improve the RC time delay related to plasma damage for the next interconnect manufacturing technology.**

***Index Terms*—Back end of line (BEOL) interconnects, porous low-k dielectric, RC delay, plasma induced damage, pulsed plasma etching.**

I. INTRODUCTION

As THE node of advanced semiconductor integrated circuits scale down further, resistance and capacitance (RC) time delays in the copper interconnection became more dominant than complementary metal oxide semiconductor (CMOS) gate delay because the smaller pitch of metal-to-metal makes the resistance and capacitance much higher [1]. In order to reduce RC time delay, conventional SiO_2 dielectric was replaced by dielectric materials with lower dielectric constant (low-k) for lower capacitance [2]. As a low-k dielectric, SiCOH film is normally used because it is easy to transfer from a SiO_2 forming method and has high thermal stability and Young's modulus. The dielectric constant of SiCOH is around 3 because a methyl group in the SiCOH makes dielectric constant low. Furthermore, in order to reduce k lower than 3, pores were introduced in the SiCOH film to have the k value lower than 2.6 and it is named as porous SiCOH. [3]–[5] However, the porous SiCOH is very easily damaged during the plasma etching processes by plasma induced damages (PIDs). That is, during the plasma etching process, plasma ions, reactive radicals, and UV/VUV photons from the plasma break Si-CH_3 bonds in SiCOH and change the material hydrophilic from hydrophobic [6]. As a result, the damaged porous SiCOH tends to make bonds with moisture easily and degrades RC time delay by making dielectric constant increased so it has been one of the most critical issues in the BEOL manufacturing technology which needs aggressive metal pitch. Detailed chemical formula and damaged structure of SiCOH after the etching are described in Figure 1.

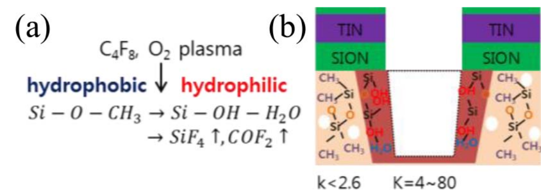

Fig. 1. (a) Chemical formula of low-k material after PID and etch byproducts (b) Structure of porous SiCOH pattern after PID.

Recently, many potential solutions to reduce the PIDs during the integration with porous SiCOH have been widely investigated using various methods such as pore stuffing [7], cryogenic etching [8], direct copper etching, etc. [9]. However, these methods are not suitable for current semiconductor manufacturing because they require additional processes, very low temperature, or a totally different integration scheme. Thus, BEOL (Back End of Line) integration with porous SiCOH still has challenges and it needs more researches to reduce the PIDs.

In conventional plasma etching processes, plasma reactor power sources are operated with a continuous wave (CW) mode for inductively coupled plasmas, capacitively coupled

Manuscript received December 18, 2019; accepted January 29, 2020. Date of publication February 3, 2020; date of current version May 5, 2020. This work was supported by the Nano Material Technology Development Program through the National Research Foundation Korea, funded by the Ministry of Education, Science, and Technology under Grant 2016M3A7B4910429. *(Corresponding author: Geun Young Yeom.)*

Jun Ki Jang, Hyun Woo Tak, Ye Ji Shin, and Doo San Kim are with the Advanced Material Science and Engineering Department, Sungkyunkwan University, Suwon 16419, South Korea.

Geun Young Yeom is with the Advanced Material Science and Engineering Department, Sungkyunkwan University, Suwon 16419, South Korea, and also with the SKKU Advanced Institute of Nano Technology, Sungkyunkwan University, Suwon 16419, South Korea (e-mail: gyyeom@skku.edu).

Color versions of one or more of the figures in this article are available online at http://ieeexplore.ieee.org.

Digital Object Identifier 10.1109/TSM.2020.2970993

0894-6507 © 2020 IEEE. Personal use is permitted, but republication/redistribution requires IEEE permission.
See https://www.ieee.org/publications/rights/index.html for more information.

Authorized licensed use limited to: Sungkyunkwan University. Downloaded on June 01,2020 at 04:34:36 UTC from IEEE Xplore. Restrictions apply.

plasmas, microwave plasmas, and electron cyclotron resonance (ECR) plasmas, etc. However, as technical nodes have been developed to much smaller sizes, the needs of advanced etching techniques have been also emerged for anisotropic profile, less PID, etc. Various techniques have been investigated such as an ion beam etching, neutral beam etching, gas pulsing etching, RF power pulsing, etc. [10]–[13] Among these, RF pulsed plasma technique has been applied in various etching areas due to easier compatibility with a conventional plasma etching process and more improvement in PID for the next generation. Compared to conventional plasma etching, by adjusting pulse frequency and duty cycle, RF pulsed plasma etching can control the plasma properties such as ion/electron density, plasma dissociation, electron temperature, etc. [13], and it can vary etch characteristics such as selectivity, etch profile, PID, uniformity in addition to UV/VUV radiation and the degree of polymerization. [14]–[19].

This study will specifically focus on the properties of RF pulsed plasma etching for less UV/VUV radiation and higher polymerization property to reduce PID of a ultra low-k dielectric material. It is reported that conventional RF plasmas using CW contain highly ionized species, highly dissociated species, and high UV/VUV radiation than RF pulsed plasma due to continuous power input to the plasma [13], [18]. Also, it is reported that the VUV penetration [20] and diffusion of F atoms [21] to low-k materials break Si-CH_3 bonding in the material and tends to damage the low-k materials. Although various pulsed plasma processes have been already applied to recent semiconductor manufacturing and several researches, they are concentrated in specific areas such as conductor etching, poly silicon etching, etc. [13]–[16] which are normally used in FEOL (Front End of Line) processes and, the effects of pulsed plasmas on the PID of low-k materials in BEOL interconnection have not been reported yet. In copper/low-k interconnection, the weakest area to PID is the sidewall of etched low-k material because the sidewall damaged layer remaining after the etching of the low-k material tends to increase the capacitance [6]. Thus, as a possible solution for the sidewall protection from the PID, RF pulsed plasma etching process which have the properties of less PID due to less UV/VUV radiation and higher polymerization to the sidewall by less ionized radicals has been investigated. To prove this hypothesis, a dual-frequency capacitively coupled plasma system (DF-CCP) with a pulsed RF source (60 MHz) and a continuous wave RF bias (2 MHz) was used and the etching properties such as etch profile, the amount of PID, etc. by using pulsed plasmas and conventional CW plasmas were compared.

II. Experimental

A. Equipment

In order to etch porous SiCOH dielectric samples, a dual frequency CCP system as shown in Figure 2 was used in the experiment.

The top and bottom electrodes were covered by a silicon plate which was surrounded by a ceramic ring for insulation. The distance between the two electrodes for RF discharge was 80mm. The top electrode was perforated for gas flow to the chamber and a 60 MHz pulsed RF power source (Pearl CF-3000) was connected to generate and control the plasma. 2 MHz RF bias power (ENI GMW-50) was connected to the bottom electrode for ion bombardment onto the substrate and was cooled by water to maintain the substrate at room temperature. Silicon substrate was located on the cooled anodized aluminum bottom electrode. And, the chamber was maintained in vacuum by using a turbo molecular pump (3200 l/s) backed by a dry pump. And, an optical emission spectrometer system (OES, Andor istar 734) was connected to the chamber by using a quartz cable to gather plasma spectra.

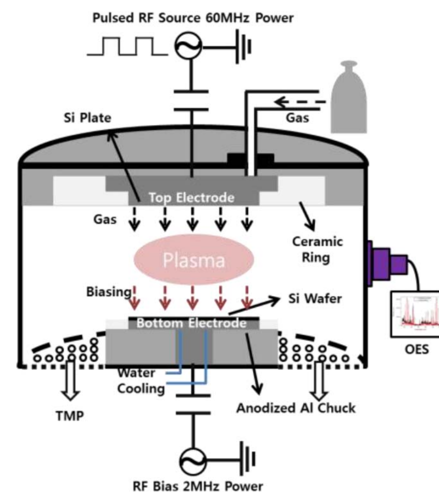

Fig. 2. Schematic diagram of a dual frequency CCP system used in this study.

Operating pressure was 30mTorr and $C_4F_8/Ar/O_2/N_2$(= 50/190/10/20 sccm) gas mixture was used. And pulsed RF power having 1 kHz frequency and 50% duty ratio which is a standard condition of pulsed plasmas [13] was applied on the top electrode(source) only while keeping the CW power to the substrate bottom electrode to generate DC bias voltage to the substrate for ion bombardment.

B. Etch Samples

A 600nm thick SiO_2 and 20nm thick SiCN layers were deposited on Si wafers for good adhesion between porous SiCOH and silicon wafer, and 150nm thick porous SiCOH(k=2.5, Porosity = 20%) was deposited on the SiCN layer. On the porous SiCOH, a SiON/TiN/SiON multilayer hard mask pattern was formed for good etch selectivity. And the porous SiCOH was etched using both CW plasmas and source pulsed plasmas. The schematic diagram of the sample for etching and RF pulsing waveforms used in the experiment are shown in Figure 3.

C. Monitoring Method

Etch profiles including etch depth, critical dimension(CD), sidewall angle of the porous SiCOH were measured by Field Emission Scanning Electron Microscopy (FE-SEM, Hitachi S-4700). The plasma damage was also characterized with FE-SEM by measuring the sidewall thickness loss before and

Authorized licensed use limited to: Sungkyunkwan University. Downloaded on June 01,2020 at 04:34:36 UTC from IEEE Xplore. Restrictions apply.

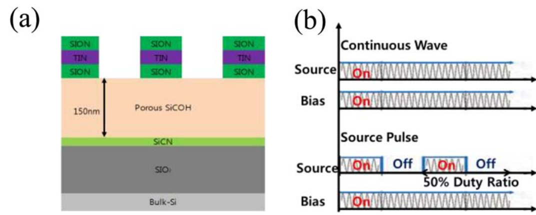

Fig. 3. Schematic diagrams of (a) a porous SiCOH pattern structure and (b) continuous wave form and pulsed wave form of RF source power used in the experiment.

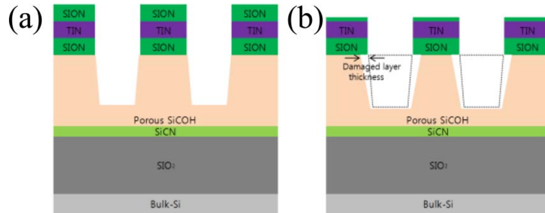

Fig. 4. Schematic diagrams of the etched SiCOH profiles (a) before and (b) after a diluted HF dipping process.

after dipping the etched samples in a diluted HF solution (0.5%, 60s). Figure 4 showed the schematic diagram of the etched profile before and after a HF dipping process for the estimation of the sidewall damage after the etching.

In addition, Fourier transform infrared spectroscopy (FT-IR Spectroscopy, Bruker Tensor 27) was measured and compared for the samples before and after the etching to monitor the peak change of porous SiCOH related to the PID and X-ray photoelectron spectroscopy (XPS, VG Microtech Inc. ESCA2000) was conducted to observe surface chemical binding peaks related to the surface polymer. The time-varying plasma characteristics such as time-varying electron density and time-varying electron temperature for the source power pulsing condition were measured by an RF filtered single Langmuir probe(ALP-150, Impedans). And, in order to observe and compare overall radicals in plasmas, a continuous mode OES was measured first, and, second, time-resolved OES was measured to monitor the change in radical intensity during pulse on and off period.

III. Results and Discussion

A. Profile Setup

Before investigating the effect of RF pulsing, the etching by using conventional continuous wave (CW) plasmas was performed to setup a proper etching condition. Figure 5 (a)–(c) show SEM images of SiCOH profiles etched with various CW RF power conditions. In order to find a proper RF power, different combinations of source and bias power were conducted and the most anisotropic profile was obtained for the condition of Figure 5 (c), which was the condition of the source 100W / bias −600V. Excessive source power (200W, Figure 5 (a)) made the etch profile less anisotropic and excessive bias voltage (−1200V, Figure 5 (b)) made the hard mask eroded more. This is related to highly dissociated reactive ions at higher powers and high ion energy bombardment for higher bias voltages. Using the plasma conditions in Figure 5 (c) and

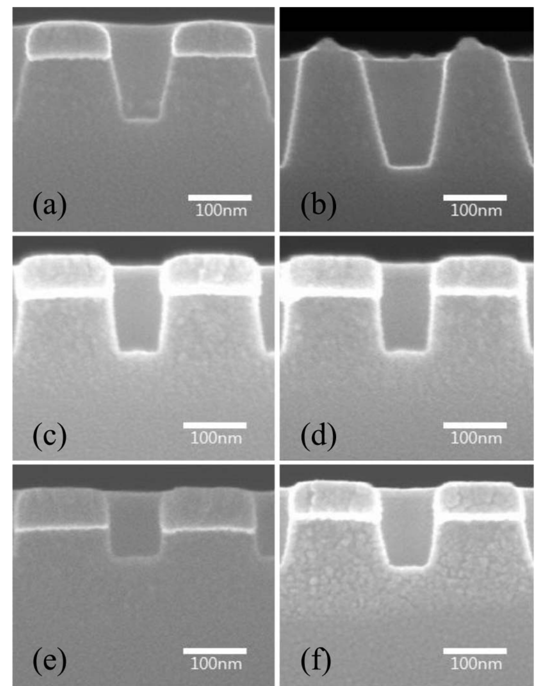

Fig. 5. SEM images of SiCOH etched profiles after the etching by (a) continuous wave / 200W source power / −600V bias voltage, (b) continuous wave / 200W source power / −1200V bias voltage, (c) continuous wave / 100W source power / −600V bias voltage, (d) source pulse /100W source power / −600V bias voltage, (e) continuous wave/ 50W source power/ −600V bias voltage, and (f) continuous wave/ 67W source power/ −600V bias voltage.

by pulsing the source power at 50% and at 1kHz, the etched profile of SiCOH as shown in Figure 5 (d) was obtained. As shown, compared to CW conditions, the etch profile for the pulse condition was more anisotropic. Detailed etch rates and sidewall slope angles of etched SiCOH for various CW source power conditions including the source pulsed power condition in Figure 5 (a) – (f) are showed in Figure 6.

In Figure 6, the data from Figure 5 (b) having the self-bias voltage of −1200V was removed all mask layer was eroded. Figure 6 (a) shows the etch rates of porous SiCOH obtained from Figure 5 (a), (c), (d), (e), and (f). Among these, the etch rate for the condition of the continuous wave / 200W source power / −600V bias voltage was the highest possibly due to the highly dissociated ion flux and, after the source power was decreased by 100W, it was dropped by 35%. On the contrary, when the pulse mode (50% at 1kHz) was turned on for the source power of 100W, the etch rate was decreased by 25%. Figure 6 (b) shows the sidewall angle of etched porous SiCOH patterns and, as shown in Figure 6 (b), the angle became more anisotropic as the source power was decreased. And, as the pulse mode was turned on, the most anisotropic etch profile was obtained for the etching condition with the source pulsing due to higher sidewall polymerization at the source pulsed condition. In the case of CW condition, RF power is continuously on, therefore, highly dissociated reactive ions and radicals are produced that make the profile less anisotropic. In addition, a thicker damaged layer is also formed (the result will be shown in the next section) due to the diffusion of radicals such as F into the SiCOH sidewall. However, In the

Authorized licensed use limited to: Sungkyunkwan University. Downloaded on June 01,2020 at 04:34:36 UTC from IEEE Xplore. Restrictions apply.

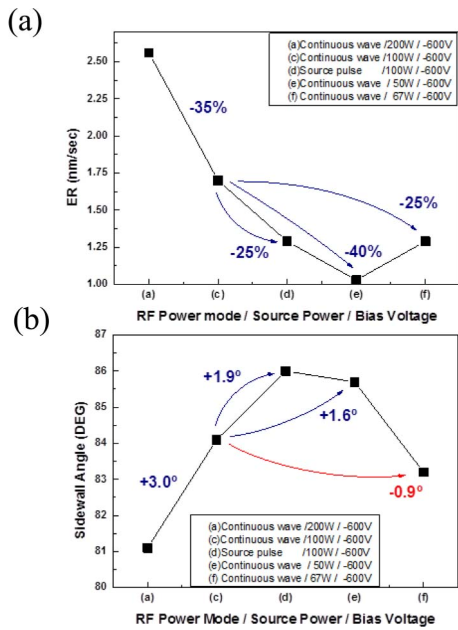

Fig. 6. (a) Etch rates and (b) measured sidewall angles for the etching of porous SiCOH etched patterns with various CW and pulse conditions.

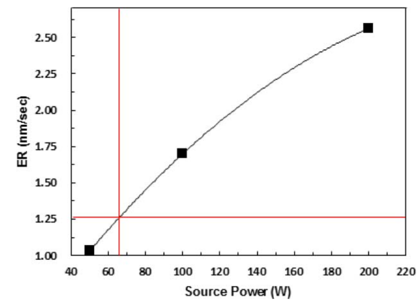

Fig. 7. Etch rate curve versus source power for CW source power conditions to calculate CW power showing similar etch rate as the pulsed source power condition (100W and 50% duty percent).

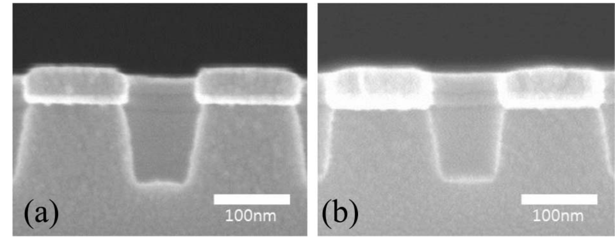

Fig. 8. SEM images of SICOH etch profiles after dipping the etched samples in a diluted HF for 60s. (a) is the profile for the CW condition (source power 100W / bias voltage −600V) and (b) is the profile for the pulsed source power condition while keeping other conditions the same as (a).

source pulsing condition, lower dissociated radicals such as CF_x are formed and recombination of F is promoted during the pulse off period, and it enhances the sidewall passivation, therefore, anisotropic profile and less sidewall damage could be obtained.

The anisotropic etch profile of the pulsed source power condition could be related to the decreased source power. Therefore, to investigate the effect of the source power condition on etch characteristics further, RF source power for the CW condition was further reduced to 50W and, the etch rate and sidewall angle were compared with the pulsed source power condition. The etch profile is showed in Figure 5 (e) and the etch rate and sidewall angle are showed on the 4th point (e) in Figure 6 (a) and (b), respectively. As shown in Figure 5 (e), the etch condition of continuous wave /50 W source power / −600V bias voltage showed a similar sidewall angle with the best condition of source pulse / 100W source power / −600V bias voltage but the etch rate was further decrease by 40% compared to the condition of continuous wave / 100W source power / −600V bias voltage while the pulsed source power condition had only 25% of etch rate drop. This result shows that the pulsed source power condition with 50% duty percentage is not just the CW source power condition with the half of source power (continuous wave / 50W source power). This is due to contribution of the etching during the source pulse off period. Because the plasma is remaining on during the pulse off period due to CW bias power and after-glow, [13] etching isn't stopped and overall etch rate is higher than the half of source power at the CW condition.

To compare the etch profiles between CW source power condition and the pulsed source power condition while the etch rates are similar each other, the CW source power having the similar etch rate as the pulsed source power condition (source pulse / 100W source power / −600V bias voltage) was calculated by drawing the etch rate as a function of CW source power and, the result is shown in Figure 7. The calculated power was 67W and the etch profile for this condition is shown in Figure 5 (f) and, also, on the last point in Figure 6(a) and (b). As shown, even though the etch depth for the condition of CW 67W source power (Fig. 5 (f)) was similar to the pulsed source power condition (Fig. 5 (d)), the sidewall angle for the CW condition was lower compared to the pulsed source power condition due to the insufficient sidewall passivation for the CW condition. Therefore, decreasing CW source power from the optimized etch condition of 100W source power not only decreased etch rate but also degraded etch profile, and, by applying source power pulsing for the optimized CW source power condition, the further improvement of etch profile could be observed.

B. Damage Characterization and Comparison

For the optimum etching condition of the CW plasma in Fig. 5 (c) and the pulsed source power condition in Fig. 5(d), plasma damage was investigated after the etching ∼100nm thick porous SiCOH. Figure 8 showed the etch profiles after dipping the etched samples in a diluted HF solution for 60 s.

As HF is normally used as a SiO_2 etchant, the plasma damaged layer on the sidewall of the etched porous SiCOH can be observed by removing the Si-O_χ layer changed from Si-CH_3 in the SiCOH surface through carbon depletion during the etch processes [22]. As shown in Fig. 8, both profiles showed the loss of a sidewall damaged layer and the sidewall angles were degraded less anisotropically. However, Figure 8 (b) showed more anisotropic profiles and lower loss of the sidewall thickness than Figure 8 (a). Detailed

Authorized licensed use limited to: Sungkyunkwan University. Downloaded on June 01,2020 at 04:34:36 UTC from IEEE Xplore. Restrictions apply.

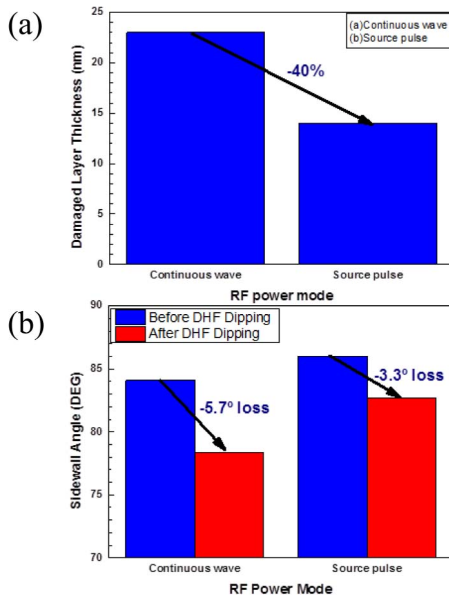

Fig. 9. (a) Damaged layer thickness and (b) sidewall angle change after dipping in a diluted HF solution.

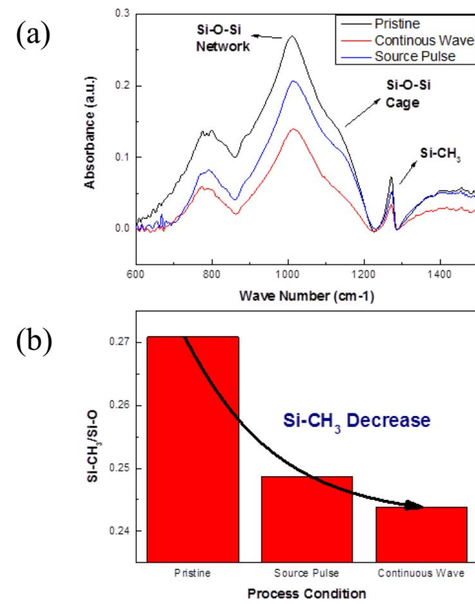

Fig. 10. (a) FT-IR spectra of porous SiCOH pattern before and after etching (b) Ratio of $Si-CH_3/Si-O$ to monitor the change of $Si-CH_3$ concentration.

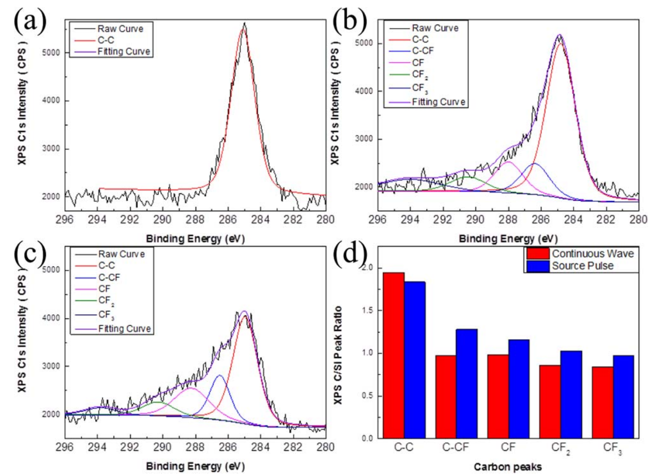

Fig. 11. XPS narrow scan data of C1s for (a) pristine porous SiCOH film, (b) etched film by using CW source power, and (c) etched film by using source pulse power mode. (d) XPS C/Si peak ratios for the comparison of each carbon binding peaks.

loss of damaged layer thickness and change in sidewall angle are shown in Figure 9. As shown in Figure 9 (a), the damaged layer thickness of the SiCOH for the pulse condition showed 40% lower value compared to that for the CW condition. Similarly, the sidewall angle change in Figure 9 (b) was less as 3.3° for the source pulse condition. These results indicate that the etching by using the RF source pulse power damages porous SiCOH less than the etching by using the CW source power due to less dissociated radicals and enhanced sidewall passivation as described in the previous section.

In order to observe the etch damage of SiCOH film more qualitatively, FT-IR analysis which is normally used for monitoring SiCOH damage [6] was performed on the pristine SiCOH samples and the SiCOH samples after etching the same depth by using CW source power and source pulse power. The samples with patterned structure were used to monitor the sidewall damage. Detailed results are shown in Figure 10. Figure 10 (a) shows FT-IR spectra and the three peaks related to the low-k structure which are 'Si-O-Si network' (near 1000 $\sim$ 1050 cm^{-1}), 'Si-O-Si cage' (near 1100 $\sim$ 1160 cm^{-1}), and '$Si-CH_3$' (near 1260 $\sim$ 1290 cm^{-1}) are shown. Among these, the peak related to the plasma damage is the peak of $Si-CH_3$ because it is related with carbon concentration in porous low-k film [6] and the $Si-CH_3$ bonding is broken when it is damaged by plasma. To compare the degree of carbon depletion in porous SiCOH accurately, the ratio of $Si-CH_3/Si-O$ was calculated for the pristine and etched samples and the results are shown in Figure 10 (b). As shown, the smaller $Si-CH_3/Si-O$ peak ratio was observed for the sample etched by the CW source power compared to that by the source pulse power even though the etch depths are the same for both samples. It indicates that the more carbon was depleted, that is, more plasma damaged for the SiCOH sample etched by the CW source power.

The less plasma damage of etched SiCOH for the source pulse power compared to the CW source power can be related to decreased F radical diffusion from the plasma to the SiCOH sidewall surface due to the higher polymerization and possibly also due to the less UV/VUV radiation during the etching for the source pulsing compared to the CW. [17]–[19], [21] Therefore, the characteristics of etched SiCOH surfaces and the characteristics of plasmas during the operation of the source pulse power condition and CW source power condition were investigated.

C. Surface and Plasma Analysis

XPS analysis on the etched SiCOH surface was carried out to observe the property of surface polymerization. The analysis was done on blanket samples. Figure 11 (a), (b), and (c) show

Authorized licensed use limited to: Sungkyunkwan University. Downloaded on June 01,2020 at 04:34:36 UTC from IEEE Xplore. Restrictions apply.

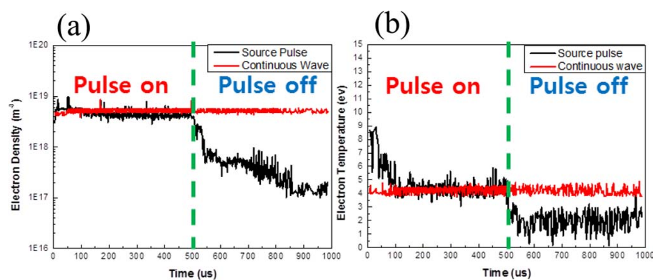

Fig. 12. Time resolved (a) electron density and (b) electron temperature for the source pulsing condition than the CW source condition. Process condition: 30mTorr and $C_4F_8/Ar/O_2/N_2$(= 50/190/10/20 sccm) gas mixture. Source power pulsing condition: 1 kHz frequency and 50% duty ratio.

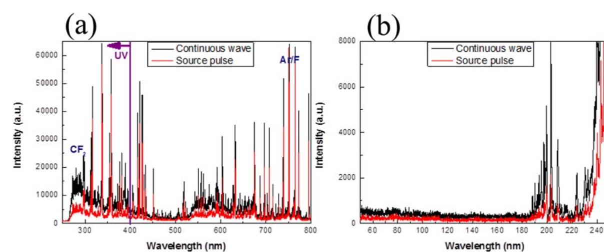

Fig. 13. (a) Continuous OES analysis for CW and source pulse condition. (b) OES analysis under 250nm wavelength region showing UV radiation ∼ 200nm (the OES system used in the experiment can measure the emission wavelength effectively from 250 ∼ 900nm due to the use of fused quartz and up to ∼200nm with much lower transmittance efficiency).

the XPS narrow scan data of C1s on the pristine SiCOH, SiCOH etched by CW source power, and SiCOH etched by source pulse power, respectively. As shown in Figure 11 (a), for the pristine film, only the carbon binding peak related to C-C peak (∼ 285 eV) was observed. But, for the SiCOH etched by the CW plasma, as shown in Figure 11 (b), additional four types of binding peaks related to surface fluorocarbon polymer such as C-CF (∼ 287 eV), CF(∼ 289 eV), CF_2(∼ 291 eV), and CF_3(∼ 294 eV) were observed [23]. In the case of SiCOH etched by the source pulse plasma, compared to SiCOH etched by CW source plasma, XPS data showed higher intensities of the binding peaks related to surface fluorocarbon polymer as shown in Figure 11 (c). For the detailed comparison of surface polymerization property, XPS carbon binding peaks were normalized to the silicon peak and the results are shown in Figure 11 (d). As shown, the degree of polymerization was higher for the source pulsing condition than the CW source condition indicating more surface fluorocarbon polymer deposition during the etch process. So the thicker fluorocarbon polymer for the source pulsing condition can protect the sidewall from the plasma damage, and which could be one of the reasons for lower SiCOH damage by the pulsed plasma. In fact, the higher polymerization for the source pulsing condition than the CW source condition is related to the lower F/CF_x (x=1,2) in the plasma by OES for the source pulsing condition than the CW source condition (as observed in Fig. 15 of the next paragraph). To explain the lower F/CF_x ratio in the plasma for the source pulsing condition, the changes in plasma characteristics during the source pulsing need to be described. Therefore, the time-varying plasma characteristics such as changes in electron density and electron temperature were measured using the $C_4F_8/Ar/O_2/N_2$(= 50/190/10/20 sccm) gas mixture for the source pulsing condition and CW source condition using a Langmuir probe and the result is shown in Fig. 12. As shown in Fig. 12, for 0∼500 μs of source power pulsing, electron density and electron temperature of CW and source pulse were similar because it's pulse power-on period except for initial electron temperature overshoot [13] required to obtain a steady state plasma from the previous pulse-off state. For 500∼1000 μs of source power pulsing, the electron density was decreased almost exponentially and the electron temperature was decreased significantly after the source pulse power off. However, the plasma was not completely turned off due to the CW bias power and possibly also due to after-glow of the plasma by 60MHz source power. Due to the lower electron density and lower electron temperature during the source power-off period, the C_4F_8 dissociates less and the dissociated F tends to recombine with CF_x and, therefore, lower F/CF_x ratio in the plasma can be obtained for the source power pulsing condition compared to CW source condition.

To observe actual dissociated species such as F, CF_x etc. and UV intensity in both plasmas, OES analysis was carried out. Two types of OES analysis were conducted by using different OES modes; the continuous mode OES which can monitor average intensity in whole wavelength region and the time-resolved mode OES which can monitor the intensity change as a function of time during the source pulse power condition. Figure 13 (a) shows the time-average OES analysis data for the process condition of CW source power and pulsed source power (100W for both CW and source pulse). For both plasma conditions, even though the peak intensities were different, similar dissociated species were distributed including species such as CF_2(near 295nm), Ar(near 751nm), and F(near 752nm). Especially, for the UV region of below 400nm, the intensity differences were larger as the wavelength was decreased indicating that the source pulse power condition radiates less UV than the CW source power condition for the same RF power. It is due to the lower fluorocarbon species emitting UV lights such as CF_2 dissociated from C_4F_8 by pulsed plasmas compared to CW plasmas. As mentioned, VUV/UV breaks $Si\text{-}CH_3$ bonds which cause low-k plasma damage, therefore, pulsed plasmas could reduce plasma damage by reducing UV radiation. Although VUV could not be observed by using a conventional OES System because VUV is absorbed in the air, but we can expect that VUV will be also decreased by using pulsed plasmas based on the results of UV and VUV light decrease investigated by Okigawa *et al.* [18]. Especially, the wavelength for Si-C bonding dissociation energy is 275nm(4.5 eV), therefore, the UV radiation by the plasmas can affect the damage to the SiCOH. In addition, as investigated by Takeda *et al.* [20], the $Si\text{-}CH_3$ bond breaking is significantly increased with the assistance of UV radiation in addition to radical diffusion.

And, for the source pulse power condition (pulse frequency of 1kHz and duty ratio of 50%), the time-resolved OES was carried out to observe the change in intensities of dissociated

Authorized licensed use limited to: Sungkyunkwan University. Downloaded on June 01,2020 at 04:34:36 UTC from IEEE Xplore. Restrictions apply.

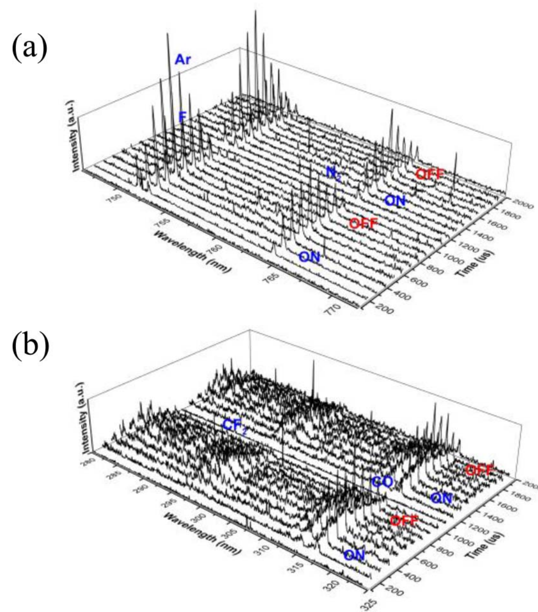

Fig. 14. Time resolved OES analysis for the wavelength range of (a) 745∼770 nm and (b) 280 ∼325 nm.

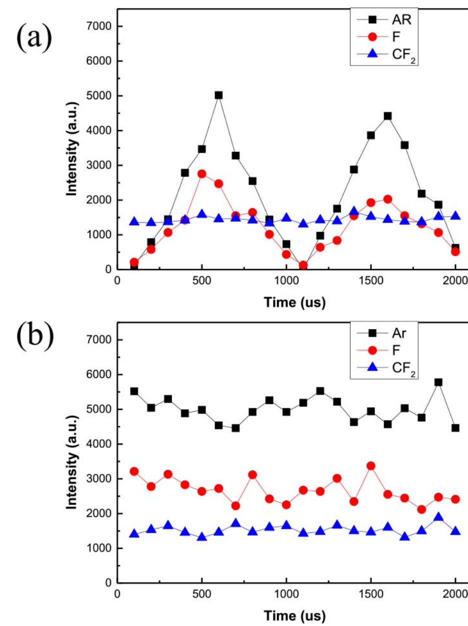

Fig. 15. OES peak intensities by time-resolved OES for (a) pulsed source power and (b) CW source power (for reference). OES peak intensities from 751 nm(Ar), 752nm(F), and 295 nm(CF_2) were taken.

species as a function of time during the pulse on/off period of the pulsed condition and the results are shown in Fig. 14 (a) for the long wavelength region of 745∼ 770 nm containing species such as Ar and F and (b) for the short wavelength region of 280∼ 325 nm containing the species such as CF_2.

Each peak intensity increased from 0 to 500 μs and then decreased from 500 to 1000 μs even though the source power was on only for 0 ∼ 500 μs. Therefore, even though the source power was off for 500 ∼1000 μs, the dissociated species were still remaining in the chamber partially due to the after-glow in the pulsed plasma. [13]–[15] And, it could be the reason why SiCOH etch rate for 100W source pulse power (50 % duty) is only 25 % lower than that for 100W of CW source power condition as in Fig. 6(a).

In order to compare the change in OES peak intensities during the pulse on/off period in Fig. 14 further, OES intensities species from Ar, F, and CF_2 in Fig. 14 were sampled and plotted as a function of time in Figure 15 (a). As a reference, the time-resolved OES intensities for the CW source power condition were also measured and are shown in Fig. 15 (b). For source pulse power condition, the OES intensities for Ar and F were significantly changed as a function of time while showing the maximum at ∼500 μs and the minimum at ∼1000 μs. On the contrary, the OES intensities related to CF_2 changed less significantly with time. Therefore, the peak intensities of Ar/F and CF_2 were reversed during the power off period. Compared to the results in Fig. 15 (a), the all the species do not change with time for the CW source power condition as shown in Fig. 15 (b) and the intensities from Ar and F were the highest in all period. F is mostly related to etching of SiCOH while CF_2 is more related to polymerization on the SiCOH surface. Therefore, a thicker surface fluorocarbon polymer was observed for the pulsed source power condition shown in Fig. 11 and it was related to the higher intensities of polymerizing dissociated species such as CF_2 in the plasma compared to the etching species such as F.

Finally, from the above observation of from the FT-IR, OES, and XPS, the mechanism of less SiCOH damage by using the source pulse power instead of CW power can be described as 1) the lower F/CF_2 in the plasma and the thicker fluorocarbon layer on the SiCOH surface during the etching decrease the diffusion of F into SiCOH sidewall which tends to break Si-CH_3 bonding at the etched sidewall surface of the SiCOH and 2) the decrease of time-average UV radiation by the source pulse RF power tends to decrease the break Si-CH_3 bonding in the SiCOH layer during the etching.

IV. Conclusion

RF source pulsed plasma etching for porous SiCOH showed more anisotropic profile and less plasma damage characteristics compared to the CW plasma etching at an optimized condition of source power 100W / bias voltage −600V. It also showed a lower damaged layer thickness and less sidewall angle change after dipping in a diluted HF solution and FTIR results showed lower carbon depletion. It was related to the higher surface polymerization properties due to higher polymerizing species in the plasma during the pulse off and possibly also due to the less UV radiation from the plasma as investigated by XPS analysis, time-resolved Langmuir probe measurement, and time-average/time-resolved OES analysis. A disadvantage of the source pulsed plasma compared to the CW plasma seems to be the etch rate drop. However, the decrease of etch rate was not significant and also the decrease of etch rate does not significantly affect the processing of next generation IC device due to the continuous scale down of the IC node. Therefore, it is believed that the RF pulsed plasmas etching can be applied a low damage etching method for the

Authorized licensed use limited to: Sungkyunkwan University. Downloaded on June 01,2020 at 04:34:36 UTC from IEEE Xplore. Restrictions apply.

advanced IC generation which needs aggressive capacitance target.

References

[1] R. H. Havemann and J. A. Hutchby, "High-performance interconnects: An integration overview," *Proc. IEEE*, vol. 89, no. 5, pp. 586–601, May. 2001, doi: 10.1109/5.929646.

[2] A. Grill, S. M. Gates, T. E. Ryan, S. V. Nguyen, and D. Priyadarshini, "Progress in the development and understanding of advanced low *k* and ultralow k dielectrics for very large-scale integrated interconnects—State of the art," *Appl. Phys. Rev.*, vol. 1, Jan. 2014, Art. no. 011306, doi: 10.1063/1.4861876.

[3] K. Maex, M. R. Baklanov, D. Shamiryan, F. Iacopi, S. H. Brongersma, and Z. S. Yanovitskaya, "Low dielectric constant materials for microelectronics," *J. Appl. Phys.*, vol. 93 no. 11, pp. 8793–8841, Jun. 2003, doi: 10.1063/1.1567460.

[4] V. McGahay, "Porous dielectrics in microelectronic wiring applications," *Materials*, vol. 3, pp. 536–562, Jan. 2010, doi: 10.3390/ma3010536.

[5] R. J. O. M. Hoofman *et al.*, "Challenges in the implementation of low-*k* dielectrics in the back-end of line," *Microelectron. Eng.*, vol. 80C, pp. 337–344, Jun. 2005, doi: 10.1016/j.mee.2005.04.088.

[6] M. R. Baklanov *et al.*, "Plasma processing of low-*k* dielectrics," *J. Appl. Phys.*, vol. 113, no. 4, pp. 1–41, Jan. 2013, doi: 10.1063/1.4765297.

[7] T. Frot *et al.*, "Post porosity plasma protection: Scaling of efficiency with porosity," *Adv. Funct. Mater.*, vol. 22, pp. 3043–3050, Apr. 2012, doi: 10.1002/adfm.201200152.

[8] L. Zhang *et al.*, "Low damage cryogenic etching of porous organosilicate low-*k* materials using $SF_6/O_2/SiF_4$," *ECS J. Solid-State Sci. Technol.*, vol. 2, no. 6, pp. N131–N139, Apr. 2013, doi: 10.1149/2.001306jss.

[9] L. Wen *et al.*, "Direct etched cu characterization for advanced interconnects,," in *Proc. IEEE Int. Interconnect Technol. Conf. (IITC)*, Grenoble, France, 2015, pp. 173–175, doi: 10.1109/IITC-MAM.2015.7325613.

[10] M. H. Jeon, K. C. Yang, J. W. Park, D. H. Yun, K. N. Kim, and G. Y. Yeom, "Etching of magnetic tunnel junction materials using reactive ion beam," *J. Nanosci. Nanotechnol.*, vol.16, no. 11, pp. 11823–11830, Mar. 2016, doi: 10.1166/jnn.2016.13602.

[11] S. Samukawa, "Ultimate top-down etching processes for future nanoscale devices: Advanced neutral-beam etching," *Jpn. J. Appl. Phys.*, vol. 45, no. 4A, pp. 2395–2407, Apr. 2006, doi: 10.1143/JJAP.45.2395.

[12] S. Sriraman and A. Paterson, "Fast gas switching for etching," U.S. Patent 13 958 239, Aug. 2, 2013.

[13] S. Banna *et al.*, "Inductively-coupled pulsed plasmas in the presence of synchronous pulsed substrate bias for robust, reliable and fine conductor etching," *IEEE Trans. Plasma Sci.*, vol. 39, no. 9, pp. 1730–1746, Sep. 2009, doi: 10.1109/TPS.2009.2028071.

[14] S. Samukawa, "Pulse-time-modulated electron cyclotron resonance plasma etching for highly selective highly anisotropic and notch-free polycrystalline silicon patterning," *Appl. Phys. Lett.*, vol. 64, no. 25, pp. 3398–3400, Jun. 1994, doi: 10.1063/1.111290.

[15] H. Ohtake, K. Noguchi, S. Samukawa, H. Lida, A. Sato, and X. Qian, "Pulse-time-modulated inductively coupled plasma etching for high-performance polysilicon patterning on thin gate oxides," *J. Vac. Sci. Technol. B, Microelectron. Process. Phenom.*, vol. 18, no. 5, pp. 2495–2499, Sep. 2000, doi: 10.1116/1.1312261.

[16] K. Tokashiki *et al.*, "Synchronous pulse plasma operation upon source and bias RFs for inductively coupled plasma for highly reliable gate etching technology," *Jpn. J. Appl. Phys.*, vol. 48, pp. 1–11, Aug. 2009, doi: 10.1143/JJAP.48.08HD01.

[17] M. Okigawa, Y. Ishikawa, and S. Samukawa, "Reduction of ultraviolet-radiation damage in SiO_2 using pulse-time-modulated plasma and its application to charge coupled 44 device image sensor processes," *J. Vac. Sci. Technol. B, Microelectron. Process. Phenom.*, vol. 21, no. 6, pp. 2448–2454, Nov. 2003, doi: 10.1116/1.1629712.

[18] M. Okigawa, Y. Ishikawa, Y. Ichihashi, and S. Samukawa, "Ultraviolet-induced damage in fluorocarbon plasma and its reduction by pulse-time-modulated plasma in charge coupled device image sensor wafer processes," *J. Vac. Sci. Technol. B, Microelectron. Process. Phenom.*, vol. 22, no. 6, pp. 2818–2822, Nov. 2004, doi: 10.1116/1.1827219.

[19] M. H. Jeon, K. C. Yang, K. N. Kim, and G. Y. Yeom, "Effect of pulse phase lag in the dual synchronized pulsed capacitive coupled plasma on the etch characteristics of SiO_2 by using a $C_4F_8/Ar/O_2$ gas mixture," *Vacuum*, vol. 121, pp. 294–299, Nov. 2015, doi: 10.1016/j.vacuum.2015.05.009.

[20] K. Takeda *et al.*, "Mechanism of plasma-induced damage to low-*k* SiOCH films during plasma ashing of organic resists," *J. Appl. Phys.*, vol. 109, no. 3, pp. 1–5, Feb. 2011, doi: 10.1063/1.3544304.

[21] E. Soda *et al.*, "Low-damage low-*k* etching with an environmentally friendly CF3I plasma," *J. Vac. Sci. Technnol. A*, vol. 26, no. 4, pp. 875–880, Jul. 2008, doi: 10.1116/1.2919137.

[22] Q. T. Le *et al.*, "Removal of plasma-modified low-*k* layer using dilute HF: Influence of concentration," *Electrochem. Solid-State Lett.*, vol. 8, no. 7, pp. F21–F24, May 2005, doi: 10.1149/1.1928234.

[23] T. Easwarakhanthan, D. Beyssen, L. L. Brizoual, and J. Bougdira, "Spectroellipsometric analysis of CHF_3 plasma-polymerized fluorocarbon films," *J. Vac. Sci. Technol. A*, vol. 24, no. 4, pp. 1036–1043, Jun. 2006, doi: 10.1116/1.2209654.

Authorized licensed use limited to: Sungkyunkwan University. Downloaded on June 01,2020 at 04:34:36 UTC from IEEE Xplore. Restrictions apply.